ELSEVIER

NeuroImage

www.elsevier.com/locate/ynimg
NeuroImage 23 (2004) 670–679

Cooperation of the anterior cingulate cortex and dorsolateral prefrontal cortex for attention shifting

Hirohito Kondo,[a,b,*] Naoyuki Osaka,[b] and Mariko Osaka[c]

[a] *Human and Information Science Laboratory, NTT Communication Science Laboratories, NTT Corporation, Atsugi 243-0198, Japan*
[b] *Department of Psychology, Graduate School of Letters, Kyoto University, Kyoto 606-8501, Japan*
[c] *Department of Psychology, Osaka University of Foreign Studies, Osaka 562-8558, Japan*

Received 10 March 2004; revised 19 May 2004; accepted 14 June 2004
Available online 12 September 2004

Attention shifting in the working memory system plays an important role in goal-oriented behavior, such as reading, reasoning, and driving, because it involves several cognitive processes. This study identified brain activity leading to individual differences in attention shifting for dual-task performance by using the group comparison approach. A large-scale pilot study was initially conducted to select suitable good and poor performers. The fMRI experiment consisted of a dual-task condition and two single-task conditions. Under the dual-task condition, participants verified the status of letters while concurrently retaining arrow orientations. The behavioral results indicated that accuracy in arrow recognition was better in the good performers than in the poor performers under the dual-task condition but not under the single-task condition. Dual-task performance showed a positive correlation with mean signal change in the right anterior cingulate cortex (ACC) and right dorsolateral prefrontal cortex (DLPFC). Structural equation modeling indicated that effective connectivity between the right ACC and right DLPFC was present in the good performers but not in the poor performers, although activations of the task-dependent posterior regions were modulated by the right ACC and right DLPFC. We conclude that individual differences in attention shifting heavily depend on the functional efficiency of the cingulo-prefrontal network.

Keywords: Attention shifting; Working memory; Anterior cingulate cortex; Dorsolateral prefrontal cortex; Structural equation modeling

Introduction

Human behavior in daily life is achieved by active maintenance of the task-relevant goal and attention shifting to several subgoals. For instance, during a drive, we can enjoy talking to a friend in the passenger seat and predict the movement of oncoming cars while keeping a destination in mind. It is assumed that goal-oriented behavior is supported by the working memory system, which consists of the domain-general central executive and domain-specific storage components (Baddeley, 1986; Baddeley and Logie, 1999). Central executive functioning includes regulation of the storage subsystems in the verbal domain (Paulesu et al., 1993; Poldrack et al., 1999) and visuospatial domain (Courtney et al., 1998; Jonides et al., 1993).

Smith and Jonides (1999) highlighted the importance of two executive functions: attention shifting for task management under a dual-task situation and inhibition of prepotent responses under a cognitive conflict situation. Neuroimaging studies have demonstrated that the anterior cingulate cortex (ACC) and dorsolateral prefrontal cortex (DLPFC) are neural bases of the central executive for dual-task performance (Bunge et al., 2000; D'Esposito et al., 1995; Smith et al., 2001) and Stroop task performance (Bush et al., 1998; MacDonald et al., 2000). To further examine the relationship between dual-task performance and the prefrontal subregions, we have used working memory tasks in which retention of several words was crossed with semantic verification of auditory and visual presented sentences (Osaka et al., 2003, 2004). It is known that these tasks show a significant correlation with reading comprehension (Daneman and Carpenter, 1980). The results indicated that the correlation of time-series fMRI data (i.e., functional connectivity) between the ACC and left DLPFC is greater for good performers than for poor performers, suggesting that synchronization between the two regions plays an important role in predicting individual differences in verbal cognitive abilities. Furthermore, Kondo et al. (2004) have demonstrated that activation of task-dependent posterior regions is regulated by the top-down control of the ACC and left DLPFC when word retention and arithmetic verification are performed concurrently. However, it is unclear how brain activity in the prefrontal regions is associated with attention shifting between visuospatial cognitive processes.

The unresolved issue is whether executive processes for attention shifting include the characteristics of hemispheric lateralization. McIntosh et al. (1994) have shown that path influences in the occipito-parietal and occipito-temporal networks of the right hemisphere are dominant in a dot-location matching task and face matching task, respectively. In addition, the dorsal and ventral pathways included stronger interactions in the right hemisphere than in the left hemisphere using structural equation modeling

* Corresponding author. Human and Information Science Laboratory, NTT Communication Science Laboratories, NTT Corporation, 3-1 Morinosato-Wakamiya, Atsugi 243-0198, Japan. Fax: +81-46-240-4716.
E-mail address: hkondo@brl.ntt.co.jp (H. Kondo).
Available online on ScienceDirect (www.sciencedirect.com.)

1053-8119/$ - see front matter © 2004 Elsevier Inc. All rights reserved.
doi:10.1016/j.neuroimage.2004.06.014

(SEM). Stephan et al. (2003) used letter- and visuospatial-decision tasks to confirm that verbal and visuospatial cognitive processes are functionally lateralized in posterior regions of the left and right hemispheres, respectively. The results indicate that the cognitive processes are controlled by the ACC in the same hemisphere. However, D'Esposito et al. (1998) have stated that working memory tasks create bilateral activation of the DLPFC, irrespective of the information modality (see also Glahn et al., 2002).

The major goal of the present study was to identify brain activity related to individual differences in attention shifting during a visuospatial working memory task. We used the rotation-arrow task to obtain dual-task performance. This working memory task requires the ability to switch controlled attention between letter verification with mental rotation and retention of arrow orientations. It is known that the rotation-arrow task is significantly correlated with visuospatial thinking rather than reading comprehension (Miyake et al., 2000; Shah and Miyake, 1996). Previous studies have found that the superior parietal lobule (SPL) and vicinity are activated during a mental rotation task (Carpenter et al., 1999; Cohen et al., 1996; Tagaris et al., 1998), whereas spatial memory has been found to be associated with activation of the premotor area (PMA) (Courtney et al., 1998; Jonides et al., 1993; Rowe et al., 2000). Thus, we determined the DLPFC, ACC, PMA, and SPL to be the regions of interest (ROIs) and compared brain activity of these ROIs between good and poor performers.

We used SEM to construct an inter-region network based on theoretical models. SEM can provide a best-fitting model that accounts for time-series fMRI data of ROIs (Büchel and Friston, 1997; Büchel et al., 1999; Bullmore et al., 2000; Honey et al., 2002; Horwitz et al., 1999; Kondo et al., 2004). We identified an estimate of effective connectivity between the ROIs with path directions in the good and poor performers. The present study tested whether activation of the posterior brain regions is modulated by the left or right hemispheric cingulo-prefrontal network.

Materials and methods

Participants

We recruited 16 participants (9 males and 7 females) from a sample of 86 college students from Kyoto, Osaka, and Nara. They were healthy, strongly right-handed, native Japanese speakers. The mean score of the Edinburgh Handedness Inventory (Oldfield, 1971) was 91.6 (range: 80–100). Their ages ranged from 22–29, with an average of 25.4. None had a previous history of any neurological or psychiatric disorders. All participants gave written informed consent, which was approved by the Institutional Review Board of NTT Communication Science Laboratories.

Before the fMRI experiment, the rotation-letter task was used to assess participants' working memory capacity for concurrent processing and storage of visuospatial information. This task is a variant of the rotation-arrow task. Each trial included a set of letters (F, J, L, P, or R) that were rotated in increments of 45° except upright (Shah and Miyake, 1996). The letters were presented for 0.2 s with an interstimulus interval (ISI) of 1.3 s. Participants were instructed to judge whether the status of letters was normal or mirror-imaged while simultaneously retaining orientations of the top of the letters. After a successive presentation of letters, a circle-shaped grid appeared with eight circles indicating the eight possible orientations. Participants selected the orientations in correct serial order by pointing a mouse cursor and pressing the left button within 2.5 s for each letter. Set sizes ranged from two to five at random, with five trials for each set size. The behavioral index was the maximal span of correctly answered responses. The mean span score for all participants was 3.29 (SD = 1.04). We selected the eight good and eight poor performers who had span scores of 4.5 and 2.5, respectively.

Behavioral tasks

Participants performed two scans (14 min 36 s for each) including three types of task epochs: Rotation + Arrow, Rotation, and Arrow conditions. The task epoch (30 s) of the Rotation + Arrow and Rotation/Arrow conditions corresponded to dual-task and single-task conditions, respectively (Fig. 1A). Participants indicated target items with their left hands using a three-key response box during a recognition epoch (16 s). Each task epoch was repeated five times within each scan, which was interlaced with a baseline epoch (16 s). The baseline epochs were established to exclude brain activation related to simple visuomotor responses.

Five letters and five arrows were alternately presented for 1.5 s with an ISI of 1.5 s under the Rotation + Arrow condition (Fig. 1B). The letters were randomly selected from 10 capitals (B, E, F, G, J, K, L, P, Q, or R) to minimize the learning effect and were rotated at 90°/−90°, 135°/−135°, and 180° for each presentation. Half of the letters were normal and the others were mirror-imaged. Arrows included eight possible orientations at 45° increments. Participants were instructed to verify whether the letters were normal or mirror-imaged by pressing either the left or right key while concurrently retaining the orientations of arrows as a sequence of spatial patterns. Five probes containing two possible

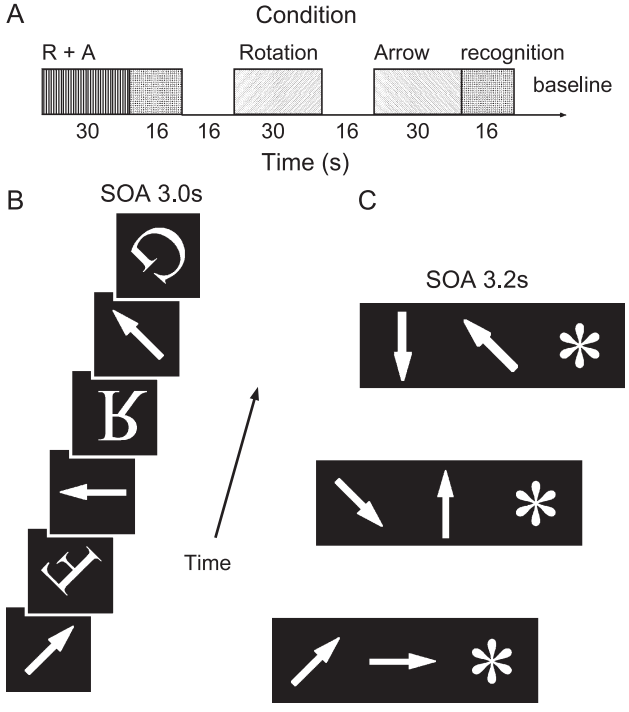

Fig. 1. Experimental design. (A) The order of task presentation was fixed. R + A: Rotation + Arrow. Schematic representation of the stimuli during the Rotation + Arrow epochs (B) and recognition epochs (C). SOA: stimulus onset asynchrony.

targets and one asterisk were successively presented for 3.0 s with an ISI of 0.2 s under the recognition epoch (Fig. 1C). Participants were asked to indicate the arrow orientations in correct serial order by pressing one of three keys on the response box. If the target did not appear, participants pressed a key corresponding to the asterisk. The chance of correctly guessing the answer was approximately 33%. The same letter and arrow were not presented within a trial.

The amount of visual input and motor response under the Rotation + Arrow condition was identical to that of the Rotation/Arrow conditions. Five letters appeared in sequence under the Rotation condition, although the arrows were replaced by a row of asterisks. Participants solely identified whether the letters were normal or mirror-imaged. Five arrows were presented under the Arrow condition, whereas letters were replaced by a pictorial signal indicating left or right. Participants pressed either the left or right key according to the signal while concurrently retaining the arrow orientations. Presentation timing of stimuli and acquisition of participants' responses under the Rotation/Arrow conditions were the same as those under the Rotation + Arrow condition. The pictorial signals were presented every 4 s during the baseline epoch, and participants pressed either the left or right key for each presentation.

The stimuli were generated from the software Presentation (Neurobehavioral Systems Inc., San Francisco, CA, USA) to synchronize with the scanner sequence. Participants could view the stimuli on a projected screen via a mirror in the head coil.

fMRI data acquisition

Brain images were obtained using a 1.5-T MRI scanner (Shimadzu-Marconi Magnex Eclipse, Shimadzu Corp., Kyoto, Japan). Head motions were minimized with a forehead strap and comfortable padding around the participant's head. Functional images (438 volumes for each scan) sensitive to blood oxygen level-dependent (BOLD) contrasts were acquired by a single-shot echo-planar imaging sequence (TR = 2 s, TE = 48 ms, flip angle = 80°, 64 × 64 at 4 mm in-plane resolution, 7-mm thickness, 20 contiguous oblique axial slices parallel to the AC–PC line). After the experimental scans, anatomical images were collected for all participants (TR = 12 ms, TE = 4.5 ms, flip angle = 20°, voxel size = 1 × 1 × 1 mm).

fMRI data analysis

Imaging data were analyzed by SPM99 (Wellcome Department of Cognitive Neurology, London, UK) and MRIcro (Rorden and Brett, 2000). Five initial images of each scan were discarded from the analysis to eliminate nonequilibrium effects of magnetization. The remaining 433 volumes of functional images were used for the subsequent analysis. The movement of all the functional images was smaller than 1 mm within each scan. Following realignment of the functional images for correction of head movement, the anatomical image was coregistered to the mean functional image. The functional images were normalized by the anatomical image and then spatially smoothed with an isotropic Gaussian filter (7-mm full-width at half-maximum).

We modeled the imaging data for each scan with the box-car function to identify significant activated voxels related to the task paradigm (the three task conditions and recognition condition). The data were high-pass filtered with maximal frequency of task alternation period (340 s) to cut off baseline drifts and low-pass filtered with a hemodynamic response function to control for temporal autocorrelation. Finally, we created four contrast images: Rotation + Arrow, Rotation, Arrow, and Rotation + Arrow vs. Rotation/Arrow. Averaged activation areas for the good and poor performers were estimated by a random-effects model. Dual-task performance created bilateral activation of the DLPFC (Brodmann's area: BA 46), ACC (BA 32), PMA (BA 6), and SPL (BA 7), which were defined as ROIs.

We computed time-series fMRI data of significant activated voxels to compare the signal intensity of these ROIs between the good and poor performers. Signal changes of local maxima were determined as a representative activation pattern of the ROIs. Based on the brain atlas (Talairach and Tournoux, 1998), ROIs were anatomically determined across each task condition for each scan, then local maxima were identified in each ROI. We used left- and right-hemisphere submaxima of the ACC because the left ACC activation was not separate from the right one for several participants. The percentage of signal changes was calculated by subtracting the average of time-series fMRI data of local maxima under the baseline condition from that under each task condition.

An individual-based regression analysis was performed to examine the relationship between signal intensity and accuracy in arrow recognition. Such a regression analysis can confirm whether the signal intensity of ROIs shows a positive or negative correlation with task performance (Bunge et al., 2001). For each scan, the percentage of signal changes was plotted as a function of accuracy in arrow recognition under the Rotation + Arrow and Rotation conditions.

The present study used SEM to identify the best-fitting structural models, which were computed by minimizing the difference between observed and predicted covariances of time-series fMRI data of ROIs in the good and poor performers. The parameters in the models were represented as a path coefficient, corresponding to an estimate of effective connectivity. Based on the procedure by Bullmore et al. (2000), the time-series fMRI data (75 volumes) under the Rotation + Arrow condition were standardized to zero mean and unit variance for each scan because task performance differed between the two groups. The data for each task epoch were temporally shifted to compensate for the delay (4 s = 2TR) of the hemodynamic response function (Honey et al., 2002). We performed a principal components analysis to calculate an average signal pattern for the good and poor performers using the standardized data. Factor loading of the first principal component was

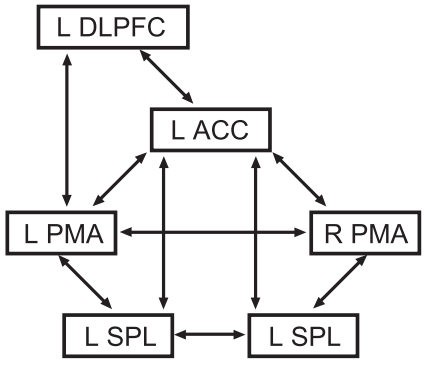

Fig. 2. Default-settings model for the left-hemisphere cingulo-prefrontal network. Regional variables and reciprocal connections are represented as rectangles and double-headed arrows. L/R DLPFC: left/right dorsolateral prefrontal cortex, ACC: anterior cingulate cortex, PMA: premotor area, SPL: superior parietal lobule.

identified in each time point. SEM was applied to create structural models based on the time-series factor loadings by a maximum likelihood method with SPSS 11.5J and Amos 4.02J software (SPSS Japan Inc., Tokyo, Japan).

We used a constrained heuristic approach to define a structural model. It is important to identify the underlying anatomical model when SEM is applied to neuroimaging data (Büchel and Friston, 1997). We initially assumed that the ACC is linked with the DLPFC and PMA and that there are reciprocal intrahemispheric connections among the ACC, PMA, and SPL (Devinsky et al, 1995). As shown in Fig. 2, either the left DLPFC and left ACC or right DLPFC and right ACC were set as the central components of attention shifting in the preferred theoretical model. Structural models were compared in terms of χ^2 statistics and differences in degrees of freedom (see Honey et al., 2002). Following the recommendation by Hu and Bentler (1998), we selected two fit indices to assess the structural models: the standardized root-mean-square residual (SRMR) and comparative fit index (CFI).

Results

Behavioral data

Fig. 3 shows the mean percentage of correctly answered responses and mean of median reaction times (RTs) in arrow recognition and letter verification. A 2 (good vs. poor performers) × 2 (dual-task vs. single-task) analysis of variance (ANOVA) on mean accuracy in arrow recognition demonstrated that the main effects of group and task conditions were significant [$F(1,14) = 11.57$, $P < 0.01$; $F(1,14) = 8.61$, $P < 0.05$, respectively]. The interaction was also significant [$F(1,14) = 21.47$, $P < 0.001$]. Post hoc analysis (Tukey's HSD test) confirmed that mean accuracy was higher for the good performers (91.0%) than for the poor performers (70.8%) under the Rotation + Arrow condition but not under the Arrow condition. Mean RTs in arrow recognition were faster for the good performers (1048 ms) than for the poor performers (1345 ms), irrespective of the task condition [$F(1,14) = 8.86$, $P < 0.01$]. These results indicate that central executive functioning for attention shifting, rather than the capacity of short-term memory per se, contributes to dual-task performance.

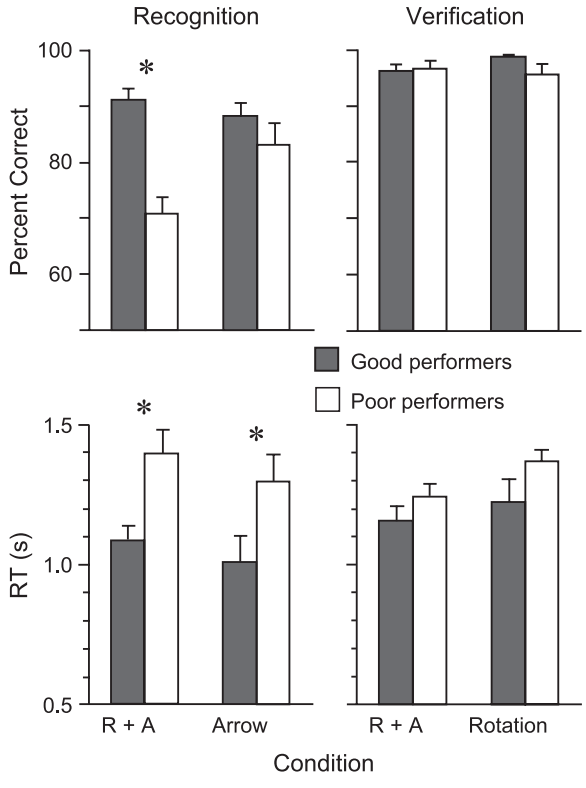

Fig. 3. Mean accuracy and mean reaction times (RTs) in arrow recognition and letter verification. Error bars indicate standard errors of means. *$P < 0.05$.

Mean accuracy and mean RTs in letter verification did not differ between the good and poor performers so that performance for each participant exceeded 90% and all responses were given within 3.0 s. Thus, it was unlikely that the performance difference in arrow recognition under the Rotation + Arrow condition was caused by a strategic trade-off of accuracy between two cognitive processes, i.e., rehearsal of arrow orientations and mental rotation for letter matching.

Performance in signal discrimination was 100% for all participants under the baseline condition. There was not a significant difference in mean RTs between the good performers (666 ms) and poor performers (733 ms) [$t(14) = 1.07$, n.s.], suggesting that the difference in dual-task performance cannot be attributed to a simple visuomotor ability.

Neuroimaging data

Dual-task specific activation was found in the bilateral DLPFC for the good and poor performers, whereas the ACC, PMA, and SPL were primarily activated under the dual-task and single-task conditions (Table 1). The activations of the two groups overlapped considerably under the Rotation + Arrow condition (Figs. 4A and B). The pattern of brain activations is consistent with the idea that attentional control is supported by a distributed network consisting of the ACC and DLPFC (Mesulam, 1990; Posner and Petersen, 1990) and previous findings that manipulation and maintenance of visuospatial representations are associated with the posterior cortex (Cohen et al., 1996; Courtney et al., 1998; Jonides et al., 1993; Tagaris et al., 1998).

Group comparison analysis was carried out to specify brain regions derived from individual differences of attention shifting (Fig. 4C). The ACC (coordinates: 2, 24, 40; $Z = 3.95$), supplementary motor area (−2, 6, 52; $Z = 3.69$), and left PMA (−44, 0, 52; $Z = 4.14$) remained when dual-task activations in the poor performers were subtracted from those in the good performers. The dorsal part of the ACC was activated in the present study, although it has recently been argued that the dorsal and rostral parts of the ACC correspond to cognitive and emotional processes, respectively (Bush et al., 2000). Two separate regions in the ventrolateral prefrontal cortex (VLPFC) (−36, 22, −18; $Z = 4.05$ and −54, 18, 10; $Z = 3.85$) were found when dual-task activations in the good performers were subtracted from those in the poor performers. There was no significant group difference in brain activity under the two single-task conditions. The results can be summarized as follows. The bilateral DLPFC was recruited for the two groups under the dual-task condition, but not under the two single-task conditions. The group difference in dual-task activation emerged in the ACC and left VLPFC.

Table 1
Brain activations across each task condition for each group

Brain region	Brodmann area	Rotation + Arrow					Rotation					Arrow				
		Coordinates			Z score	Voxels	Coordinates			Z score	Voxels	Coordinates			Z score	Voxels
		x	y	z			x	y	z			x	y	z		
Good performers																
Prefrontal cortex	L46	−46	38	6	5.04	43										
	R46	44	44	6	4.25	31										
Anterior cingulate cortex	L32/8	−6	26	42	5.15	191	−4	28	42	4.39		−4	36	34	4.41	
	R32/8	6	32	36	4.98		4	32	38	4.73	114	6	28	38	4.63	89
Premotor area	L6	−30	8	50	6.27	1643	−28	12	52	6.92	51	−28	4	44	6.38	1476
	R6	28	8	48	4.68	294						26	20	40	5.53	464
Superior parietal lobule	L7	−26	−50	50	5.87	2626	−38	−42	58	5.51	728	−36	−44	58	6.75	2838
	R7	14	−60	56	6.23	2200	38	−40	60	4.41	338	16	−58	56	5.77	1894
Inferior temporal cortex	L37	−46	−60	−2	5.11	41	−46	−58	−8	4.73	233	−46	−62	−4	4.39	31
	R37	48	−56	−4	5.83	325	50	−54	−6	6.84	198	48	−56	−4	4.61	30
Visual association cortex	L18/19	−26	−90	12	6.11	774	−32	−92	4	5.36	381					
	R18/19	38	−82	4	4.78	601	30	−88	8	5.26	543					
Cerebellum	L	−30	−72	−44	4.68	73						−18	−72	−44	4.95	101
	R	14	−72	−40	5.11	284						12	−72	−44	5.30	432
Poor performers																
Prefrontal cortex	L46	−40	36	10	4.05	18										
	R46	40	38	6	4.15	14										
Anterior cingulate cortex	L32/8	−4	16	50	5.85	618	−4	20	50	4.82	69	−4	20	44	6.44	941
	R32/8	4	22	42	5.29							6	26	40	5.36	
Premotor area	L6	−4	16	50	5.85	1266	−28	2	48	5.27	266	−30	8	54	6.87	1220
	R6	24	6	52	5.40	326	26	2	50	4.32	35	24	6	56	6.24	408
Superior parietal lobule	L7	−28	−48	52	6.46	2709	−28	−50	54	5.04	607	−20	−64	52	6.45	2105
	R7	24	−64	56	6.94	2059	30	−52	52	4.94	79	24	−62	56	6.67	1601
Inferior temporal cortex	L37	−50	−62	−4	4.49	214	−50	−62	−4	5.30	375	−52	−66	2	4.73	28
	R37	48	−66	−6	5.33	622	48	−60	−6	5.77	464					
Visual association cortex	L18/19						−40	−78	−4	5.25	319					
	R18/19						38	−80	2	5.59	325					
Cerebellum	R	38	−62	−24	6.53	64						34	−58	−28	5.03	99
Thalamus	L	−10	−4	14	5.00	311										

Note. Activation is significant at $P < 0.05$ of cluster level ($Z > 3.72$), corrected for multiple comparison.

Table 2 shows the mean percentage of signal changes for the good and poor performers under the three task conditions. A 2 (group) × 3 (task) ANOVA demonstrated that mean signal change in the left DLPFC was greater under either the Rotation + Arrow or Arrow condition than under the Rotation condition [$F(2,60) = 14.51$, $P < 0.001$]. However, the group difference did not reach a significant level. In the right DLPFC, the main effect of the task condition and interaction were significant [$F(2,60) = 7.99$, $P < 0.001$; $F(2,60) = 4.02$, $P < 0.05$]. Post hoc analysis confirmed that mean signal change was greater for the good performers than for the poor performers under the Rotation + Arrow condition but not under either the Rotation or Arrow condition. The pattern of the results in the left and right ACC was similar to that in the left and right DLPFC. The main effects of the group and task conditions and interaction were significant in the right ACC [$F(1,30) = 8.05$, $P < 0.01$; $F(2,60) = 15.58$, $P < 0.001$; $F(2,60) = 3.32$, $P < 0.05$, respectively], while the main effect of the task condition was only significant in the left ACC [$F(2,60) = 24.55$, $P < 0.001$]. Mean signal change in the right ACC was greater for the good performers than for the poor performers under the Rotation + Arrow condition but not under either the Rotation or Arrow condition. In the left/right PMA and left/right SPL, the main effect of the task condition was significant [$F(2,60) = 89.93$, 66.80, 75.43, and 88.44, $P < 0.001$, respectively]. The pattern of signal changes in the right ACC and right DLPFC was consistent with the interaction of arrow recognition between the group and task conditions.

We performed an individual-based regression analysis to further examine the differences of signal intensity between the Rotation + Arrow and Arrow conditions (Fig. 5). Dual-task performance showed a significant positive correlation with signal change in the right DLPFC and right ACC [$r(30) = 0.49$ and 0.49, $P < 0.05$], although the correlation in the left DLPFC and left ACC was relatively small [$r(30) = -0.01$ and 0.23, n.s.]. Single-task performance was significantly correlated with signal change in the right PMA [$r(30) = 0.52$, $P < 0.01$] but not that in the left PMA [$r(30) = 0.15$, n.s.]. These results suggest that signal intensity in the right DLPFC and right ACC is a crucial factor in predicting individual differences of dual-task performance.

We searched for the best-fitting models of the good and poor performers by using SEM, then compared path directions and effective connectivity in the models between the two groups. First, when the left DLPFC and left ACC were set as an attentional controller, the best model for the good performers was obtained as follows: left DLPFC → left PMA; left ACC → left SPL; right PMA → left PMA; and left PMA → left SPL (Model A_1 in Table 3). For the poor performers, we identified the following structure as the best model: left DLPFC; left ACC → left PMA; left PMA → right PMA; and right PMA → right SPL (Model B_1). Second, we

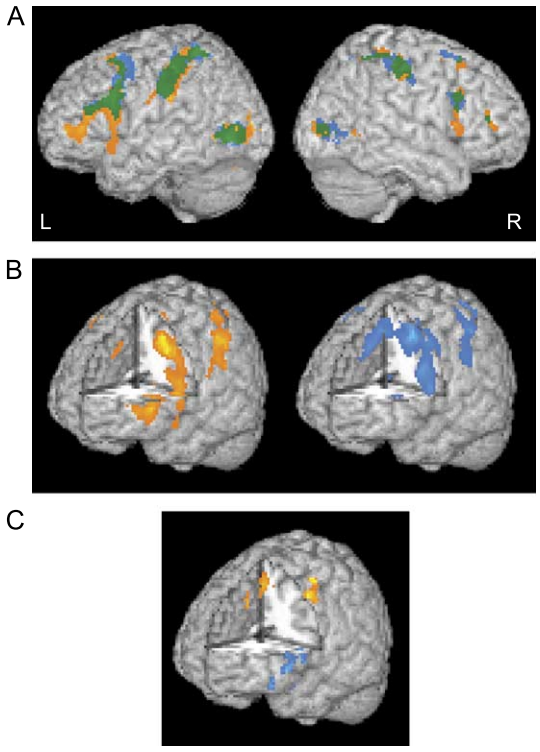

Fig. 4. Averaged activation areas of good performers (yellow) and poor performers (blue) under dual-task condition at uncorrected $P < 0.001$ of voxel level. (A) Green regions indicate common activations of the two groups. (B) A portion of the brain was cut out on a point (coordinates: 0, 12, 12) of the median plane. (C) Direct comparison of dual-task activation between the two groups.

produced the best-fitting models for the good performers (Model A_2) and poor performers (Model B_2) in which activations of the PMA and SPL were modulated by the right DLPFC and right ACC (see also Figs. 6A and B). The χ^2 difference test confirmed that Model A_2 was a better fit than Model A_1 [$\chi^2(1) = 5.41$, $P < 0.01$]. The SRMR and CFI of Model A_2 reached a satisfactory level. All of the indices of Model B_2 were better than those of Model B_1. When a path from the right DLPFC to right ACC was added in Model B_2, the addition did not significantly improve the fit of the model [$\chi^2(1) = 2.35$, $P > 0.05$]. Thus, fit indices of the right hemispheric cingulo-prefrontal network were better than those of the left hemispheric cingulo-prefrontal network in the two groups.

Table 2
Mean signal change of ROIs across each task condition for each group

Brain region		Rotation + Arrow		Rotation		Arrow	
		Good	Poor	Good	Poor	Good	Poor
Prefrontal cortex	L	0.81	0.77	0.40	0.29	0.60	0.66
	R	0.77	0.47	0.36	0.38	0.55	0.60
Anterior cingulate cortex	L	0.95	0.80	0.39	0.33	0.77	0.66
	R	0.86	0.63	0.45	0.32	0.63	0.57
Premotor area	L	1.32	1.23	0.49	0.38	1.69	1.65
	R	0.98	1.01	0.30	0.42	1.00	0.90
Superior parietal lobule	L	1.78	1.65	0.66	0.49	1.69	1.65
	R	1.53	1.57	0.63	0.53	1.47	1.31

Note. Good: good performers, Poor: poor performers.

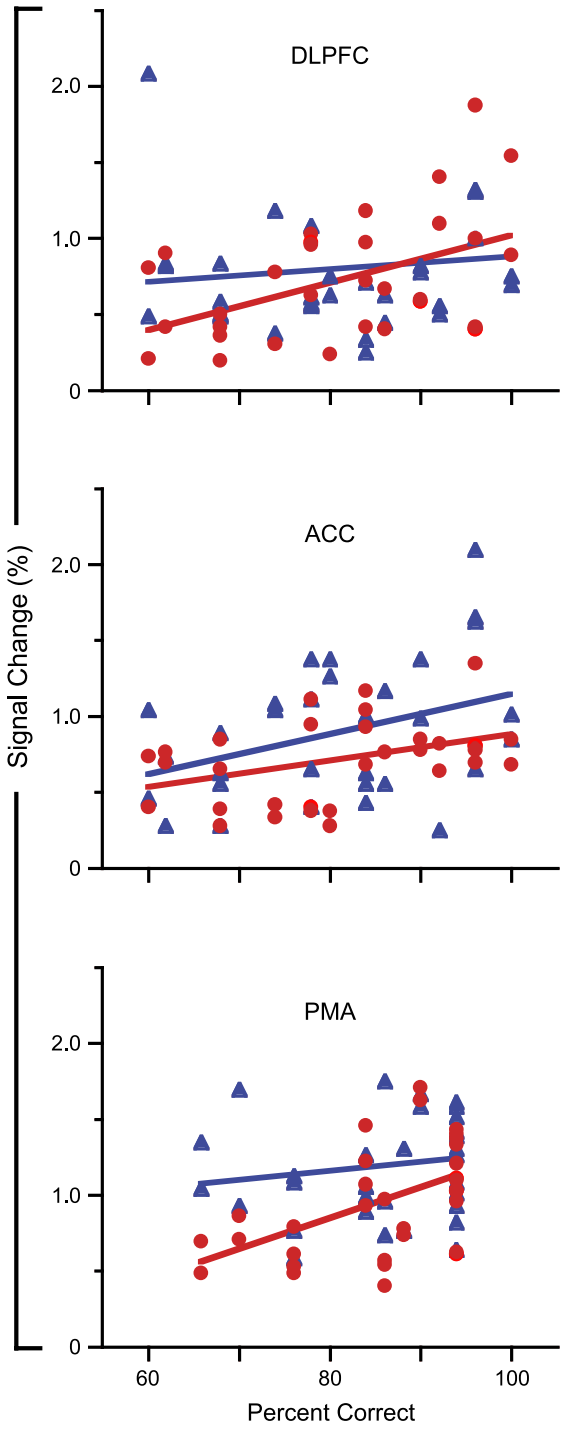

Fig. 5. Scatter plots showing correlations between mean signal change and accuracy in arrow recognition ($N = 32$). Top and middle panels show data under the Rotation + Arrow condition, while bottom panel shows data under the Arrow condition. Blue triangles and red circles represent the results of the left and right hemispheres, respectively.

We found several differences between Model A_2 and B_2. First, the functional connection from the right DLPFC to right ACC was present in the good performers but not in the poor performers. The estimate of effective connectivity in Model A_2 was 0.28, with a 95% confidence interval (CI) of −0.02 to 0.52. Second, there was a difference in sign between prefrontal and posterior subregions,

Table 3
Fit indices for structural models

Model	*df*	χ^2	*P*	χ^2/df	SRMR	CFI
Good performers						
A_1 (left DLPFC and left ACC)	6	17.00	0.009	2.83	0.124	0.800
A_2 (right DLPFC and right ACC)	5	11.59	0.041	2.32	0.099	0.934
Poor performers						
B_1 (left DLPFC and left ACC)	7	19.43	0.007	2.78	0.094	0.841
B_2 (right DLPFC and right ACC)	7	15.03	0.036	2.15	0.127	0.884

Note. SRMR, standardized root-mean-square residual; CFI, comparative fit index. Nonsignificant χ^2 statistics and $\chi^2/df < 2$ represent a good fit. SRMR < 0.080 and CFI > 0.950 indicate a better fit.

namely, a negative influence in the good performers and positive influence in the poor performers. Finally, top-down influences from the prefrontal regions to the posterior regions were relatively greater in the good performers than in the poor performers. Path influence of the right DLPFC on the right PMA was −0.54 (95% CI: −0.38 to −0.68) in Model A_2, while it was 0.21 (95% CI: 0.01–0.37) in Model B_2. Path influence of the right ACC on the left SPL was −0.55 (95% CI: −0.37 to −0.73) in Model A_2, whereas the influence from the right ACC to the right SPL was 0.27 (95% CI: 0.04–0.53) in Model B_2.

Discussion

This neuroimaging study demonstrates that attention shifting between the visuospatial cognitive processes is modulated by top-down control of the ACC and DLPFC, particularly in the right hemisphere. We found bilateral activation of the DLPFC in the good and poor performers under the dual-task condition but not under the single-task condition. Regression analysis confirmed that signal intensity of the right ACC and right DLPFC showed a positive correlation with dual-task performance. SEM showed the best-fitting model where activations of task-dependent posterior regions are regulated by the right hemispheric cingulo-prefrontal network. However, effective connectivity between the right ACC and right DLPFC was present in the good performers but not in the poor performers. The present study contributes to our better understanding of brain systems for attention shifting, cognitive control, and intelligence in humans.

Activations related to manipulation and maintenance of spatial information

Mental rotation for letter matching created activations of the bilateral PMA, SPL, inferior temporal cortex, and visual association cortex for the good and poor performers. The brain activity did not reflect visuomotor responses for judgment because the effect was removed by the baseline condition. Previous studies have demonstrated that the mental rotation of 2-D and 3-D objects is associated with the parieto-occipital network (Cohen et al., 1996; Tagaris et al., 1998) and pointed out that the amount of activation in the bilateral intraparietal sulcus increases as the degree of mental rotation increases (Carpenter et al., 1999). Thus, it seems that the SPL and surrounding areas play a critical role in the transformation of spatial coordinates, such as mental rotation.

Mean signal change in the DLPFC, ACC, PMA, and SPL was lower under the Rotation condition than under the Arrow condition. The reason may be that mental rotation includes intermittent cognitive processes for manipulation of representations, although sustained cognitive processes are required during rehearsal of spatial patterns. It is unlikely that the difference was derived from additional demand for signal discrimination under the Arrow condition. Although Kondo et al. (2004) used a task paradigm similar to that used in the present study, signal intensity in all ROIs in that study was lower under the storage-oriented (word retention) condition than under the processing-oriented (arithmetic verification) condition. The behavioral results showed that mean RTs for letter matching were approximately 1.3 s, whereas those for arithmetic verification were 2.6 s, suggesting that the increase of signal changes depends on the number of cognitive steps in processing requirements rather than on small demand of detection task.

Visuospatial rehearsal processes produced activations of the ACC, PMA, and SPL. Mean signal change in the right PMA was positively correlated with single-task performance in arrow recognition. These results indicate that spatial memory for delayed responses is based on the PMA. Neurophysiological studies of monkeys have shown that neurons in the DLPFC surrounding the principal sulcus are associated with spatial memory in saccadic eye movement (Funahashi et al., 1989, 1993). However, neuroimaging studies of humans have demonstrated that the PMA is responsible for spatial memory of object location (Jonides et al., 1993; Rowe et al., 2000). Courtney et al. (1998) also indicated that sustained activity during spatial memory delay is recruited in the bilateral posterior part of the superior frontal sulcus but that the activation does not depend on eye movement, suggesting that the brain region specialized for spatial memory is situated more superior and posterior in the frontal lobe in humans than in monkeys. Thus, it seems that the internal representation of visual input is generated from the visual association cortex and inferior temporal cortex, spatial coordinates of the representation are estimated in the SPL, and the representation is temporarily maintained in the PMA (see also McIntosh et al., 1994).

Individual differences in attention shifting for task management

The present study demonstrated that the right ACC and right DLPFC, rather than the PMA and SPL, contribute to attention shifting for dual-task management. Accuracy in arrow recognition was greater for the good performers than for the poor performers under the dual-task condition but not under the single-task condi-

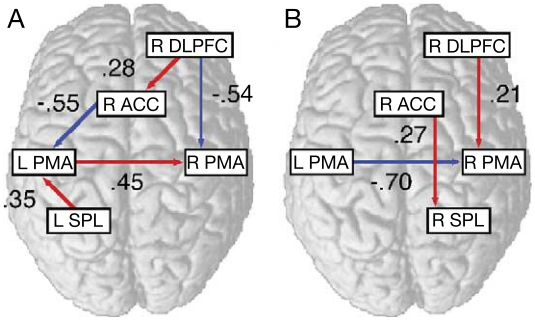

Fig. 6. Structural equation modeling. The best-fitting models for the good performers (A) and poor performers (B), corresponding to Models A_2 and B_2 in Table 3. All path coefficients are significant ($P < 0.05$). See legend of Fig. 2 for abbreviations.

tion, suggesting that the group difference heavily depends on attention shifting rather than the capacity of short-term memory. The behavioral interaction was consistent with the activation pattern where mean signal change of the right ACC and right DLPFC was positively correlated with dual-task performance but not with single-task performance. The medial prefrontal regions and left VLPFC were activated by direct comparison of dual-task activation in the good and poor performers, respectively, but the DLPFC did not remain. There is the possibility that the ACC and DLPFC play different roles in attention shifting between verification of letter status and retention of arrow orientations.

SEM confirmed that effective connectivity from the right DLPFC to the right ACC is an important factor in predicting individual differences in dual-task performance. Absolute values of effective connectivity from the ACC and DLPFC to the PMA and SPL were greater in the good performers than in the poor performers. Furthermore, time-series signal changes of the posterior regions were suppressed by those of the prefrontal regions in the good performers but not in the poor performers. This trend was also observed during a verbal working memory task (Kondo et al., 2004). The results indicate that closer cooperation between the ACC and DLPFC is strongly related to attention shifting and that the cingulo-prefrontal network allocates attentional resources to cognitive processes in the task-dependent regions.

The finding that activations for task-dependent processes are regulated by cooperation between the ACC and DLPFC is consistent with the concept of the hierarchical model in which inhibition control during the Stroop task is mediated by the two brain regions (Botvinick et al., 2001; Cohen et al., 2000). It is assumed that the Stroop task includes executive processes for resolution of cognitive conflict because participants are asked to name the color when the word "red" is presented in green type. The model postulates that the ACC and DLPFC play critical roles in performance monitoring for decision making and selective attention for task-relevant responses, respectively. The DLPFC and motor area are modulated by the ACC via the locus coeruleus. Response output from the motor area provides the ACC with feedback. The similarity of these findings suggests that several executive processes are controlled by the degree of effective connectivity from either the ACC or DLPFC to the posterior regions.

Previous studies have demonstrated that the ACC is responsible for evaluative processes, such as performance monitoring, error detection, and resolution of response conflict (Botvinick et al., 1999; Bush et al., 1998; Carter et al., 1998; MacDonald et al., 2000). The ACC is properly positioned to monitor information flow in the brain so that it includes abundant reciprocal connections to the motor system and limbic system (Devinsky et al., 1995). Also, from the findings of a lesion study (Damasio, 1999) and neurophysiological study (LeDoux, 1996), it appears that the ACC is a critical part of an inner alert system that binds emotions and actions together into goal-oriented behavior. The DLPFC is related to executive processes, such as the coordination of concurrent cognitive processes and selective attention for task-relevant information (Cohen et al., 1997; D'Esposito et al., 1995; MacDonald et al., 2000; Rowe et al., 2000). The fact that each brain region includes several cognitive functions suggests the possibility that cognitive control depends on changes in individual and collaborative activities of the ACC and DLPFC. Thus, general fluid intelligence in humans may be caused by the functional integration of the alert system based on the ACC and the executive system based on the DLPFC (see also Duncan et al., 2000; Gray et al., 2003).

A potential criticism could be that the cooperation between the ACC and DLPFC may arise for other reasons. One possibility is that the good performers overlearned the rotation-arrow task, compared with the poor performers. However, all participants were naive with respect to the working memory task. Although Raichle et al. (1994) argued that activations in the ACC and DLPFC deteriorate once automatic cognitive processes are established during a verb generation task, we did not find any indication that mean signal change in the two regions was greater for the poor performers than for the good performers. Thus, it is unlikely that the synchronization of the two regions simply reflects the learning effect. Another possibility is that the group difference is related to the degree of mental effort. However, it is unlikely that the poor performers were unable to concentrate on the current task because mean accuracy in arrow recognition was approximately 70%. Cowan (2001) has demonstrated that we can memorize three to four items under dual-task situations. We therefore do not believe that the difference of activations was solely caused by the mental effort factor.

Hemispheric asymmetry of executive processes in the prefrontal regions

The good and poor performers shared similarity in that the best-fitting model includes the right-hemisphere cingulo-prefrontal network. There is the possibility that the left DLPFC is functionally independent of the attentional control system in visuospatial working memory, although we found dual-task specific activation in the bilateral DLPFC. In contrast, previous studies have shown that cooperation between the ACC and left DLPFC is related to dual-task performance when word retention is combined with either sentence verification (Osaka et al., 2003, 2004) or arithmetic verification (Kondo et al., 2004). As highlighted by Stephan et al. (2003), these results indicate that the requirement of the left and right cingulo-prefrontal networks varies with the modality of the internal representations to be manipulated and remembered.

However, a different view is that demanding task-management creates bilateral activation of the DLPFC, irrespective of the information modality (D'Esposito et al., 1998). Rypma et al. (1999) have suggested that additional bilateral activation in the DLPFC is recruited when the recruitment of verbal working memory task exceeds the capacity of phonological memory in the left inferior frontal cortex. Furthermore, Newman et al. (2002) argued that the right DLPFC is involved in strategic planning for the integration of information during a verbal reasoning task (see also Prabhakaran et al., 2000).

From the perspective of executive processes, behavioral studies demonstrate the functional asymmetry between verbal and visuospatial working memory. In the verbal domain, Engle et al. (1999) examined whether working memory (i.e., processing and storage) tasks are separate from short-term memory (i.e., storage-oriented) tasks using SEM. The results indicated that structures of the two memory systems are highly related yet separable. When the common memory factor was removed from working memory and short-term memory, the residual factor of working memory showed a significant correlation with general fluid intelligence, but that of short-term memory did not. Thus, it was concluded that the residual factor of working memory reflects executive processes and that a major difference between working memory and short-term memory is caused by the differential involvement of the central executive. In contrast, Miyake et al. (2001) argued that working

memory and short-term memory for the visuospatial domain are not clearly separable. Taken together, the data indicate that visuospatial working memory tasks impose a considerably greater demand on the central executive than verbal working memory tasks. Thus, there is the possibility that the severe limited capacity in the visuospatial domain causes diverse activations of the DLPFC so that the visuospatial system is not as well-established as the phonological system in the brain. It is at least our contention that the activation of the right ACC and right DLPFC is more important for switching attention between visuospatial cognitive processes than that of the left ACC and left DLPFC.

Conclusion

The behavioral interaction between the group and task conditions was consistent with the imaging data showing that mean signal change in the right ACC and right DLPFC was greater in the good performers than in the poor performers under the dual-task condition but not under the single-task condition. SEM indicated that activations of task-dependent regions are regulated by the right ACC and right DLPFC and that cooperation between the two brain regions is closely related to better performance of visuospatial working memory. We conclude that individual differences in attention shifting for cognitive control heavily depend on the functional efficiency of the cingulo-prefrontal network.

Acknowledgments

We thank two anonymous reviewers and Makio Kashino for their thoughtful comments on an early version of this article, Noboru Sugamura for administrative support, and Takanori Kochiyama for statistical advice. This work was supported by research grants from the Kyoto University 21st Century Center of Excellence Program, the 29th Nissan Science Foundation, and the Japan Ministry of Education, Culture, Sport, Science and Technology (12301005 and 14310041).

References

Baddeley, A.D., 1986. Working Memory. Oxford Univ. Press, New York.

Baddeley, A.D., Logie, R.H., 1999. Working memory: the multiple-component model. In: Miyake, A., Shah, P. (Eds.), Models of Working Memory: Mechanisms of Active Maintenance and Executive Control. Cambridge Univ. Press, New York, pp. 28–61.

Botvinick, M., Nystrom, L.E., Fissell, K., Carter, C.S., Cohen, J.D., 1999. Conflict monitoring versus selection-for-action in anterior cingulate cortex. Nature 402, 179–181.

Botvinick, M.M., Braver, T.S., Barch, D.M., Carter, C.S., Cohen, J.D., 2001. Conflict monitoring and cognitive control. Psychol. Rev. 108, 624–652.

Büchel, C., Friston, K.J., 1997. Modulation of connectivity in visual pathways by attention: cortical interactions evaluated with structural equation modelling and fMRI. Cereb. Cortex 7, 768–778.

Büchel, C., Coull, J.T., Friston, K.J., 1999. The predictive value of changes in effective connectivity for human learning. Science 283, 1538–1541.

Bullmore, E., Horwitz, B., Honey, G., Brammer, M., Williams, S., Sharma, T., 2000. How good is good enough in path analysis of fMRI data? NeuroImage 11, 289–301.

Bunge, S.A., Klingberg, T., Jacobsen, R.B., Gabrieli, J.D.E., 2000. A resource model of the neural basis of executive working memory. Proc. Natl. Acad. Sci. U. S. A. 97, 3573–3578.

Bunge, S.A., Ochsner, K.N., Desmond, J.E., Glover, G.H., Gabrieli, J.D.E., 2001. Prefrontal regions involved in keeping information in and out of mind. Brain 124, 2074–2086.

Bush, G., Whalen, P.J., Rosen, B.R., Jenike, M.A., Mclnerney, S.C., Rauch, S.L., 1998. The counting stroop: an interference task specialized for functional neuroimaging-validation study with functional MRI. Hum. Brain Mapp. 6, 270–282.

Bush, G., Luu, P., Posner, M.I., 2000. Cognitive and emotional influences in anterior cingulate cortex. Trends Cogn. Sci. 4, 215–222.

Carpenter, P.A., Just, M.A., Keller, T.A., Eddy, W., Thulborn, K., 1999. Graded functional activation in the visuospatial system with the amount of task demand. J. Cogn. Neurosci. 11, 9–24.

Carter, C.S., Braver, T.S., Barch, D.M., Botvinick, M.M., Noll, D., Cohen, J.D., 1998. Anterior cingulate cortex, error detection, and the online monitoring of performance. Science 280, 747–749.

Cohen, M.S., Kosslyn, S.M., Breiter, H.C., DiGirolamo, G.J., Thompson, W.L., Anderson, A.K., Bookheimer, S.Y., Rosen, B.R., Belliveau, J.W., 1996. Changes in cortical activity during mental rotation: a mapping study using functional MRI. Brain 119, 89–100.

Cohen, J.D., Perlstein, W.M., Braver, T.S., Nystrom, L.E., Noll, D.C., Jonides, J., Smith, E.E., 1997. Temporal dynamics of brain activation during a working memory task. Nature 386, 604–608.

Cohen, J.D., Botvinick, M., Carter, C.S., 2000. Anterior cingulate and prefrontal cortex: who's in control. Nat. Neurosci. 3, 421–423.

Courtney, S.M., Petit, L., Maisog, J.M., Ungerleider, L.G., Haxby, J.V., 1998. An area specialized for spatial working memory in human frontal cortex. Science 279, 1347–1350.

Cowan, N., 2001. The magical number 4 in short-term memory: a reconsideration of mental storage capacity. Behav. Brain Sci. 24, 87–114.

Damasio, A.R., 1999. The Feeling of What Happens: Body and Emotion in the Making of Consciousness. Harcourt Brace, New York.

Daneman, M., Carpenter, P.A., 1980. Individual differences in working memory and reading. J. Verbal Learn. Verbal Behav. 19, 450–466.

D'Esposito, M., Detre, J.A., Alsop, D.C., Shin, R.K., Atlas, S., Grossman, M., 1995. The neural basis of the central executive system of working memory. Nature 378, 279–281.

D'Esposito, M., Aguirre, G.K., Zarahn, E., Ballard, D., Shin, R.K., Lease, J., 1998. Functional MRI studies of spatial and nonspatial working memory. Cognit. Brain Res. 7, 1–13.

Devinsky, O., Morrell, M.J., Vogt, B.A., 1995. Contributions of anterior cingulate cortex to behaviour. Brain 118, 279–306.

Duncan, J., Seitz, R.J., Kolodny, J., Bor, D., Herzog, H., Ahmed, A., Newell, F.N., Emslie, H., 2000. A neural basis for general intelligence. Science 289, 457–460.

Engle, R.W., Tuholski, S.W., Laughlin, J.E., Conway, A.R.A., 1999. Working memory, short-term memory, and general fluid intelligence: a latent-variable approach. J. Exp. Psychol. Gen. 128, 309–331.

Funahashi, S., Bruce, C.J., Goldman-Rakic, P.S., 1989. Mnemonic coding of visual space in the monkey's dorsolateral prefrontal cortex. J. Neurophysiol. 61, 331–349.

Funahashi, S., Chafee, M.V., Goldman-Rakic, P.S., 1993. Prefrontal neuronal activity in rhesus monkeys performing a delayed anti-saccade task. Nature 365, 753–756.

Glahn, D.C., Kim, J., Cohen, M.S., Poutanen, V.-P., Therman, S., Bava, S., Van Erp, T.G.M., Manninen, M., Huttunen, M., Lönnqvist, J., Standertskjöld-Nordenstam, C.G., Cannon, T.D., 2002. Maintenance and manipulation in spatial working memory: dissociations in the prefrontal cortex. NeuroImage 17, 201–213.

Gray, J.R., Chabris, C.F., Braver, T.S., 2003. Neural mechanisms of general fluid intelligence. Nat. Neurosci. 6, 316–322.

Honey, G.D., Fu, C.H.Y., Kim, J., Brammer, M.J., Croudace, T.J., Suckling, J., Pich, E.M., Williams, S.C.R., Bullmore, E.T., 2002. Effects of verbal working memory load on corticocortical connectivity modeled by path analysis of functional magnetic resonance imaging data. NeuroImage 17, 573–782.

Horwitz, B., Tagamets, M.-A., McIntosh, A.R., 1999. Neural modeling, functional brain imaging, and cognition. Trends Cogn. Sci. 3, 91–98.

Hu, L., Bentler, P.M., 1998. Fit indices in covariance structure modeling: sensitivity to underparameterized model misspecification. Psychol. Methods 3, 424–453.

Jonides, J., Smith, E.E., Koeppe, R.A., Awh, E., Minoshima, S., Mintun, M.A., 1993. Spatial working memory in humans as revealed by PET. Nature 363, 623–625.

Kondo, H., Morishita, M., Osaka, N., Osaka, M., Fukuyama, H., Shibasaki, H., 2004. Functional roles of the cingulo-frontal network in performance on working memory. NeuroImage 21, 2–14.

LeDoux, J., 1996. The Emotional Brain: The Mysterious Underpinnings of Emotional Life. Simon and Schuster, New York.

MacDonald III, A.W., Cohen, J.D., Stenger, V.A., Carter, C.S., 2000. Dissociating the role of the dorsolateral prefrontal and anterior cingulate cortex in cognitive control. Science 288, 1835–1838.

McIntosh, A.R., Grady, C.L., Ungerleider, L.G., Haxby, J.V., Rapoport, S.I., Horwitz, B., 1994. Network analysis of cortical visual pathways mapped with PET. J. Neurosci. 14, 655–666.

Mesulam, M.M., 1990. Large-scale neurocognitive networks and distributed processing for attention, language, and memory. Ann. Neurol. 28, 597–613.

Miyake, A., Friedman, N.P., Emerson, M.J., Witzki, A.H., Howerter, A., Wager, T.D., 2000. The unity and diversity of executive functions and their contributions to complex "frontal lobe" tasks: a latent variable analysis. Cognit. Psychol. 41, 49–100.

Miyake, A., Friedman, N.P., Rettinger, D.A., Shah, P., Hegarty, M., 2001. How are visuospatial working memory, executive functioning, and spatial abilities related? A latent-variable analysis. J. Exp. Psychol. Gen. 130, 621–640.

Newman, S.D., Just, M.A., Carpenter, P.A., 2002. The synchronization of the human cortical working memory network. NeuroImage 15, 810–822.

Oldfield, R.C., 1971. The assessment and analysis of handedness: the Edinburgh inventory. Neuropsychologia 9, 97–113.

Osaka, M., Osaka, N., Kondo, H., Morishita, M., Fukuyama, H., Aso, T., Shibasaki, H., 2003. The neural basis of individual differences in working memory capacity: an fMRI study. NeuroImage 18, 789–797.

Osaka, N., Osaka, M., Kondo, H., Morishita, M., Fukuyama, H., Shibasaki, H., 2004. The neural basis of executive function in working memory: an fMRI study based on individual differences. NeuroImage 21, 623–631.

Paulesu, E., Frith, C.D., Frackowiak, R.S., 1993. The neural correlates of the verbal component of working memory. Nature 362, 342–345.

Poldrack, R.A., Wagner, A.D., Prull, M.W., Desmond, J.E., Glover, G.H., Gabrieli, J.D., 1999. Functional specialization for semantic and phonological processing in the left inferior prefrontal cortex. NeuroImage 10, 15–35.

Posner, M.I., Petersen, S.E., 1990. The attention system of the human brain. Annu. Rev. Neurosci. 13, 25–42.

Prabhakaran, V., Narayanan, K., Zhao, Z., Gabrieli, J.D., 2000. Integration of diverse information in working memory within the frontal lobe. Nat. Neurosci. 3, 85–90.

Raichle, M.E., Fiez, J.A., Videen, T.O., MacLeod, A.-M.K., Pardo, J.V., Fox, P.T., Petersen, S.E., 1994. Practice-related changes in human brain functional anatomy during nonmotor learning. Cereb. Cortex 4, 8–26.

Rorden, C., Brett, M., 2000. Stereotaxic display of brain lesions. Behav. Neurol. 12, 191–200.

Rowe, J.B., Toni, I., Josephs, O., Frackowiak, R.S., Passingham, R.E., 2000. The prefrontal cortex: response selection or maintenance within working memory? Science 288, 1656–1660.

Rypma, B., Prabhakaran, V., Desmond, J.E., Glover, G.H., Gabrieli, J.D., 1999. Load-dependent roles of frontal brain regions in the maintenance of working memory. NeuroImage 9, 216–226.

Shah, P., Miyake, A., 1996. The separability of working memory resources for spatial thinking and language processing: an individual differences approach. J. Exp. Psychol. Gen. 125, 4–27.

Smith, E.E., Jonides, J., 1999. Storage and executive processes in the frontal lobes. Science 283, 1657–1661.

Smith, E.E., Geva, A., Jonides, J., Miller, A., Reuter-Lorenz, P., Koeppe, R.A., 2001. The neural basis of task-switching in working memory: effects of performance and aging. Proc. Natl. Acad. Sci. U. S. A. 98, 2095–2100.

Stephan, K.E., Marshall, J.C., Friston, K.J., Rowe, J.B., Ritzl, A., Zilles, K., Fink, G.R., 2003. Lateralized cognitive processes and lateralized task control in the human brain. Science 18, 384–386.

Tagaris, G.A., Richter, W., Kim, S.-G., Pellizzer, G., Andersen, P., Ugurbil, K., Georgopoulos, A.P., 1998. Functional magnetic resonance imaging of mental rotation and memory scanning: a multidimensional scaling analysis of brain activation patterns. Brain Res. Rev. 26, 106–112.

Talairach, J., Tournoux, P., 1998. Co-planar Stereotaxic Atlas of the Human Brain. Thieme, Stuttugart.